Draft version July 27, 2016
Preprint typeset using LaTeX style AASTeX6 v. 1.0

arXiv:1607.07699v1 [astro-ph.GA] 26 Jul 2016

A HIGH-VELOCITY CLOUD IMPACT FORMING A SUPERSHELL IN THE MILKY WAY

Geumsook Park and Bon-Chul Koo
Department of Physics and Astronomy, Seoul National University
Seoul 151-747, Korea

Ji-hyun Kang
Korea Astronomy and Space Science Institute
Daejeon 305-348, Korea

Steven J. Gibson
Department of Physics and Astronomy, Western Kentucky University
1906 College Heights Blvd., Bowling Green, KY 42101, USA

J. E. G. Peek
Space Telescope Science Institute
3700 San Martin Dr., Baltimore, MD 21218, USA

Kevin A. Douglas
Department of Physics and Astronomy, Okanagan College
1000 K. L. O. Rd., Kelowna, British Columbia V1Y 4X8, Canada

Eric J. Korpela
Space Sciences Laboratory, University of California
Berkeley, CA 94720, USA

Carl E. Heiles
Radio Astronomy Lab, UC Berkeley
601 Campbell Hall, Berkeley, CA 94720, USA

ABSTRACT

Neutral atomic hydrogen (HI) gas in interstellar space is largely organized into filaments, loops, and shells, the most prominent of which are "supershells". These gigantic structures requiring $\gtrsim 3\times 10^{52}$ erg to form are generally thought to be produced by either the explosion of multiple supernovae (SNe) in OB associations or alternatively by the impact of high-velocity clouds (HVCs) falling to the Galactic disk. Here we report the detection of a kiloparsec (kpc)-size supershell in the outskirts of the Milky Way with the compact HVC 040+01−282 (hereafter CHVC040) at its geometrical center using the "Inner-Galaxy Arecibo L-band Feed Array" HI 21-cm survey data. The morphological and physical properties of both objects suggest that CHVC040, which is either a fragment of a nearby disrupted galaxy or a cloud originated from an intergalactic accreting flow, collided with the disk ~ 5 Myrs ago to form the supershell. Our result shows that some compact HVCs can survive their trip through the Galactic halo and inject energy and momentum into the Milky Way disk.

Keywords: Galaxy: disk — ISM: clouds — radio lines: ISM

1. INTRODUCTION

Supershells are large gaseous shells of radius greater than a few hundred parsecs. They are distinct from other shell-like structures in their extraordinarily large energy requirement, i.e., $\gtrsim 3 \times 10^{52}$ erg, which corresponds to $\gtrsim 30$ supernova (SN) explosions (Heiles 1979, 1984; McClure-Griffiths et al. 2002). About twenty supershells have been found in the Milky Way, and numerous neutral atomic hydrogen (HI) holes corresponding to supershells have been discovered in nearby dwarfs and spiral galaxies (Kamphuis et al. 1991; Bagetakos et al. 2011). These gigantic structures are generally thought to arise from multiple SN explosions in stellar OB associations. But most supershells are missing a stellar association in their interior, and the number of supershells and their energies are usually incompatible with the level of star formation in those galaxies (Heiles 1984; Rhode et al. 1999). Therefore, several alternative scenarios have been proposed, the most popular of which is the collision of high-velocity clouds (HVCs) with the disk (Tenorio-Tagle 1980; Tenorio-Tagle et al. 1987; Mirabel & Morras 1990).

HVCs are HI clouds with radial velocities very different from the disk material in the Milky Way, e.g., with a deviation more than 50 $\mathrm{km\,s^{-1}}$ from the range of permitted velocities in a simple model of the distribution and rotation of the HI gas in the Galaxy (Wakker 1991). Some large HVC complexes are known to be gas streams tidally stripped from satellite galaxies of the Milky Way, but the origin of isolated compact HVCs (CHVCs) remain controversial: they could be clouds formed from galactic fountain or intergalactic accreting flows, part of the large HVC complexes, or condensations in the multi-phase circumgalactic medium (Putman et al. 2011; Wakker 2004; Putman et al. 2012). The HVC origin has been proposed for a few supershells (Heiles 1984; Mirabel & Morras 1990; Tamanaha 1997), but there has been no clear example showing a direct link between the two, particularly for CHVCs.

Here we report the detection of a Galactic supershell with an associated HVC, GS040.2+00.6−70 (hereafter GS040). GS040 was first identified as a faint, forbidden-velocity wing feature (FVW 40.0+0.5) in the low-resolution, large-scale longitude-velocity study of Kang & Koo (2007). We have found that GS040 appears to be a complete circular ring with complicated structures inside in our high-resolution I-GALFA (Inner-Galaxy ALFA) HI 21-cm line survey data. The I-GALFA survey is a survey of the first Galactic quadrant visible to Arecibo ($\ell = 32^\circ$ to 77° and $|b| \lesssim 15^\circ$) done by using the 7-beam Arecibo L-band Feed Array (ALFA) receiver on the Arecibo 305 m telescope, and it provides sensitive ($\Delta T_b = 0.2$ K) and fully-sampled HI maps at spatial and spectral resolutions of $4'$ and 0.184 $\mathrm{km\,s^{-1}}$, respectively (Koo et al. 2010; Gibson et al. 2012). The I-GALFA survey data further reveal that there is a CHVC at the very center of GS040. This CHVC, named HVC 040+01−282 (hereafter CHVC040), was first identified in the Leiden/Dwingeloo survey (Wakker & van Woerden 1991) and was later classified as an isolated CHVC by Braun & Burton (1999) and de Heij et al. (2002). Westmeier et al. (2005) presented a higher-resolution ($9'$) HI image obtained from the Effelsberg telescope, which showed that CHVC040 has a pronounced head-tail structure. Our Arecibo HI images reveal detailed spatial and velocity structure of CHVC040 strongly suggesting its association with the supershell GS040. We describe two structures in Section 2, and discuss their physical characteristics and their association together with some implications on the disruption of HVCs in Section 3.

2. SUPERSHELL GS040.2+00.6−70 AND HIGH-VELOCITY CLOUD HVC040+01−282

The supershell GS040 is centered at $(\ell, b) = (40.^\circ2, +0.^\circ6)$ and clearly visible from $v_{\rm LSR} \sim -120$ to -70 $\mathrm{km\,s^{-1}}$. In an integrated intensity map (Figure 1), GS040 appears as a complete circular ring of radius $\sim 1.^\circ3$ with complicated structures inside. More detailed structures can be seen in Figure 2, which presents velocity channel maps. At the most negative velocities (~ -120 $\mathrm{km\,s^{-1}}$), we see diffuse emission with embedded knotty filaments near the center and an extended filament in the south[1]. The features are observable at even more negative velocities (-150 $\mathrm{km\,s^{-1}} < v_{\rm LSR} < -120$ $\mathrm{km\,s^{-1}}$) but they are extremely weak and hard to detect in velocity-channel maps. As the velocity increases ($v_{\rm LSR} \gtrsim -90$ $\mathrm{km\,s^{-1}}$), the nebulosity fades out, and a larger ($\sim 2.^\circ6$) ring structure appears, which resembles a cartwheel with a bright central "hub" and several "spokes" (see also Figure 1). The size of the ring increases slightly with velocity indicating that the ring structure is an approaching portion of an expanding shell. At velocities greater than about -70 $\mathrm{km\,s^{-1}}$, the Galactic background HI emission becomes dominant, and the emission associated with GS040 is less clear.

At the very center of GS040 is the HVC CHVC040. The positional coincidence of CHVC040 with the GS040's central hub is striking as can be seen in Figure 3, which is the position-velocity map crossing the center of GS040. The morphological agreement between the two is also noticeable. Our high-resolution Arecibo HI image reveals that CHVC040 has a blunt cone shape with a steep southwestern boundary and a faint envelope flaring out northeast

[1] Directions in this paper are all in reference to Galactic coordinates, not J2000 Equatorial coordinates.

(Figure 4). This morphology of CHVC040 matches well with that of the central hub of GS040, e.g., see Figure 1 and also the channel map at -88 km s^{-1} in Figure 2.

Figure 4 shows the detailed spatial and velocity structures of CHVC040. The integrated intensity map in the left frame shows that CHVC040 has a bright, $\sim 12' \times 15'$- sized "core" elongated along the northeast-southwest direction. The core appears to be composed of several clumps with a sharp boundary at southwest, whereas the diffuse envelope appears to be slightly more extended toward southeast. The mean HI column density, assuming that the emission is optically thin, is 1.5×10^{19} cm^{-2} while the peak HI column density is about two times higher. The velocity centroid map in the middle frame shows that systemic velocity attains its most negative ($\lesssim -290$ km s^{-1}) at the southwestern boundary and most positive (~ -260 km s^{-1}) along the southeastern boundary and also in the middle of the northwestern boundary. The mean systematic velocity is -282 km s^{-1}. If the most positive feature in the northwestern boundary were not present, the velocity structure could have been suggestive of a rotation with respect to the northeast-southwest symmetry axis at speed of $\lesssim 20$ km s^{-1}. The velocity width (Full Width at Half Maximum; FWHM) ranges 25–45 km s^{-1} over most parts of the cloud with a median of 36 km s^{-1}. The southwesternmost thin layer has relatively narrow width ($\sim$19–28 km s^{-1}) while parts of the northern area has width $\gtrsim 50$ km s^{-1}. The region with the narrowest line width is very thin ($\sim 3'$), and therefore Westmeier et al. (2005) could not spatially resolve it.

Some representative line profiles are shown in Figure 5 together with the average line profile of the cloud. Most profiles are well described with a single Gaussian component, while some profiles, e.g., c and e-g, show clear double peaks or a narrow component superposed on a broad component. The velocity width of the mean profile is 45 km s^{-1}, which is considerably larger than the median value (36 km s^{-1}) of individual profiles, presumably due to the dispersion of central velocities. The median width corresponds to a kinetic temperature of 2.8×10^4 K. At several positions, narrow velocity components are detected, but still their widths are ≥ 10 km s^{-1}, which implies a kinetic temperature $\geq$ 2,000 K. This indicates that CHVC040 is mostly composed of warm neutral gas, which is not unusual for CHVCs (Winkel et al. 2011; Faridani et al. 2014). But it is different from those head-tail HVCs with a narrow-line head of undisturbed cold HI gas and a wide-line tail of disturbed warm HI gas (e.g., HVC125+41-207; Brüns et al. 2001).

3. DISCUSSION

3.1. *Formation of GS040 by the Collision of CHVC040*

The location of CHVC040 at the geometrical center of GS040 suggests that their physical association is very likely. The centroids of the CHVC emission and that of the GS040's hub emission overlap within $\sim$ 0.2 degrees. The probability of this being a random alignment is $\sim 3 \times 10^{-6}$, and multiplying this by $\sim$ 300 CHVCs yields an overall probability of 9×10^{-4} for any CHVC aligning this well with the GS040's hub. No intermediate-velocity HI connecting the two is apparent (Figure 3), but this could be because the gas is ionized. We searched for a warm ionized gas associated with GS040 using the Wisconsin Hα Mapper Northern Sky Survey (WHAM-NSS) data (Haffner et al. 2003). The survey has an angular resolution of 1°, and, around the GS040 area, it provides Hα spectra covering $v_{\rm LSR}$ from -85 to $+100$ km s^{-1} at spectral resolutions of 12 km s^{-1}. We have examined the Hα intensity map integrated over the velocity range of GS040 (-85 to -66 km s^{-1}), but could not detect an associated emission ($\lesssim$ 0.05 R where $1R = 10^6/4\pi$ photons cm^{-2} sr^{-1} s^{-1}). Note that this area is bright in the total Hα intensity map with a mean intensity of about 3 R, so that we do not expect to see the faint emission associated with either GS040 or CHVC040 in the all-sky Hα maps (Finkbeiner 2003; Dennison et al. 1998). We also searched for an associated hot ionized gas using the 0.1-2.4 keV image of the ROSAT All-Sky X-ray Survey (1 pixel scale = 44″; Voges et al. 1999), but couldn't detect any emission.

CHVC040 belongs to the "Galactic Center Negative" (GCN) HVC complex, which is a collection of small discrete HVCs sparsely distributed over a $70° \times 70°$ area within $\ell = 0°$ to 70° and $b = -60°$ to 10° (Wakker & van Woerden 1991; Winkel et al. 2011). A kinematic model has been proposed where GCN is a smooth gas flow starting at $b = -60°$ at a heliocentric distance of 35 kpc and crossing the Galactic plane obliquely at 15 kpc (Jin 2010). For comparison, GS040 is probably located near the Scutum-Centaurus (Sct-Cen) arm at a distance of $\sim$ 20 kpc (Dame & Thaddeus 2011) because the disrupted interstellar medium (ISM) is seen only at velocities below that of the Sct-Cen arm (~ -60 km s^{-1}), not at higher velocities (see Figures 2 and 3). We examined lists of known stellar objects, HII regions, OB stars, and SN remnants (SNRs), but no known sources are likely to be associated with GS040. There is one HII region (G039.864 + 00.645) in the *WISE* catalog of Galactic HII regions (Anderson et al. 2014) that is located at $\sim 6'$ west of the hub. But this HII region has a systematic velocity of -40.9 km s^{-1} (Anderson et al. 2011) and is enclosed by a small (68″) dust shell, so it cannot be responsible for the HI shell. Instead the distance of $\sim$ 20 kpc is not unreasonable for CHVC040, because GCN does not have a smooth extended envelope like other HVC complexes,

and it appears to be composed of several subpopulations that do not share a common origin (Winkel et al. 2011). Note that the geometrical center of GS040 is well below the Galactic plane ($\sim 420\,d_{20}$ pc where $d_{20} \equiv d/20$ kpc), i.e., at $b = +0.^{\circ}6$ while the midplane there is at $b \sim +1.^{\circ}8$ because the Galactic plane is warped in the outer Galaxy (Levine et al. 2006). It is difficult to imagine the SN origin for a supershell at such height, and CHVC040 is most likely the energy/momentum source for GS040.

The total energy deposited (E_E) in the Galactic disk by CHVC040 can be inferred from the parameters of the GS040 supershell. The radius of GS040 is $450\,d_{20}$ pc, while its mass at $v_{\rm LSR} \leq -75$ km s^{-1} is $1.6 \times 10^5\,d_{20}^2\ M_\odot$ including the cosmic abundance of helium. If we account for the mass unobservable due to Galactic background HI emission, the total mass of GS040 would be considerably greater. Adopting $v_s \sim 30$ km s^{-1} as the expansion speed of the shell, its kinetic energy is $E_K \gtrsim 1.4 \times 10^{51}\,d_{20}^2$ erg. The collision should have occurred $\sim (1/3)R_s/v_s \sim 5 \times 10^6\,d_{20}$ yr ago, where the numerical factor 1/3 accounts for the deceleration of the shell. Note that E_K is a small fraction of the total energy deposited (E_E), most of which should have been radiated away. If GS040 was produced by multiple SNe, then, assuming instantaneous energy injection (Heiles 1979), $E_E \sim 5.3 \times 10^{43}\,n_0^{1.12}\,R_s^{3.12}\,v_s^{1.4} \sim 1.2 \times 10^{53}\,(n_0/0.1\ {\rm cm}^{-3})$ erg, where n_0 is ambient hydrogen density. At the position of GS040, the mean HI density in the midplane is $\sim 0.1\,{\rm cm}^{-3}$, and the HI scale height is about 720 pc (Levine et al. 2006). So $n_0 \sim 0.06$ cm^{-3}, and we have $E_E \sim 7 \times 10^{52}$ erg. For comparison, the total extent of CHVC040 is $210\,d_{20} \times 320\,d_{20}$ pc^2 while its HI mass is $M_{\rm CHVC} = 5{,}800\,d_{20}^2\ M_\odot$. The area used to derive this mass has a geometrical mean radius of 150 pc, so that the mean hydrogen density of CHVC040 is 0.017 cm^{-3}. If CHVC040 collided with the rotating disk with the mean 'deviation' speed (absolute difference in velocity from the disk gas there) of HVCs, i.e., ~ 240 km s^{-1} (Wakker 2004), the kinetic energy and momentum would be $4.7 \times 10^{51}\,d_{20}^2$ ergs and $2.0 \times 10^6\,d_{20}^2\ M_\odot$km s^{-1} including the He abundance, respectively. This implies that the mass of CHVC040 when it collided with the disk should have been an order of magnitude greater and that the HVC that we see (CHVC040) might be the remains of the original HVC.

The spatial morphology and velocity structure of CHVC040 suggest that it is moving southwest in the plane of the sky and is approaching us. The steep southwestern boundary of the cloud might represent the region compressed by the interaction with the ambient medium, whereas the diffuse envelope might be the material stripped off from the cloud due to the interaction or by the ram pressure of the surrounding medium (Santillán et al. 1999; Kwak et al. 2009). The small velocity width along the southwestern boundary and large velocity width beyond appear to be consistent with such speculation. Recently, Heitsch et al. (2016) suggested that, for a CHVC with head-tail structure, the inclination angle, i.e., the angle between the CHVC's trajectory and the line-of-sight, can be derived from the asymmetry in position-velocity diagram along the head-tail line crossing the center of mass. The morphology of CHVC040 is different from typical head-tail CHVCs, i.e., CHVC040 has a wide flaring 'tail' not a narrow elongated tail (see also § 2), and its core is fragmented, so that it is not obvious if their model can be applied. Nevertheless if we assume that the center of mass is near the southwestern boundary and apply their model (their equations 1–4) to the position-velocity diagram along the red-dashed line in Figure 1, we obtain an inclination angle of $\sim 30^\circ$ which is consistent with our expectation.

The shape of CHVC040 appears to be pointed away from the Galactic midplane as if it already went through the midplane. But the geometrical center of the supershell coincides with the current location of CHVC040, not being located in the midplane. Perhaps CHVC040 is approaching at an angle to the warped Galactic disk and has not yet fully penetrated the disk to the midplane. It is worth to note that, according to the Jin (2010)'s model, the GCN HVC stream is colliding to the Galactic plane almost perpendicularly *from below*, while the head-tail directions of individual HVCs seem to indicate that there is no preferential direction in their motions (Winkel et al. 2011). Therefore, the orbit of CHVC040 is uncertain. The colliding geometry and the origin of the complex structures such as the hub and spokes in GS040 need to be explored.

3.2. *CHVC040 and Disruption of HVCs*

There are about three hundred known CHVCs in the Milky Way (de Heij et al. 2002; Putman et al. 2002). A considerable fraction of CHVCs has a head-tail structure indicating a ram pressure interaction with the diffuse galactic halo gas (Putman et al. 2011). An important question is whether they are totally dissipated in the Galactic halo to feed the multi-phase circumgalactic medium or they can survive their trip through the halo (e.g., Putman et al. 2011). Since CHVC040 is located in the far outer Galaxy, it may be of extragalactic origin rather than originating from a Galactic fountain, although it is not clear whether CHVC040 was originally a fragment of a nearby tidally disrupted galaxy or a cold cloud formed in a larger accreting flow of ionized, low-metallicity intergalactic gas. Our result then directly shows that at least some CHVCs of extragalactic origin do survive and collide with the Galactic disk. According to numerical studies, CHVCs with HI masses $\lesssim 3 \times 10^4\ M_\odot$ would be totally disrupted in the Galactic

halo unless they are embedded in dark matter (Heitsch & Putman 2009; Plöckinger & Hensler 2012). But dynamical shielding by an extended diffuse gaseous component can significantly extend their lifetime (Putman et al. 2012). We have checked whether there are additional sources like the CHVC040-GS040 system in the I-GALFA HI data using the HVC catalog of de Heij et al. (2002). There are twelve CHVCs in their Table 2 including CHVC040 in the I-GALFA survey area, most of which are at relatively high latitudes. They are isolated HVCs and have $v_{\rm LSR} < -150$ km s^{-1}, so they belong to the GCN HVC complex. We see low-velocity HI features around some CHVCs, but none of them appear associated. A systematic study against all CHVCs may reveal other CHVC-supershell systems.

This work was supported by the National Research Foundation of Korea (NRF) grant funded by the Korea Government (MSIP) (No. 2012R1A4A1028713).

REFERENCES

Anderson, L. D., Bania, T. M., Balser, D. S., & Rood, R. T. 2011, ApJS, 194, 32

Anderson, L. D., Bania, T. M., Balser, D. S., et al. 2014, ApJS, 212, 1

Bagetakos, I., Brinks, E., Walter, F., et al. 2011, AJ, 141, 23

Braun, R., & Burton, W. B. 1999, A&A, 341, 437

Brüns, C., Kerp, J., & Pagels, A. 2001, A&A, 370, L26

Dame, T. M., & Thaddeus, P. 2011, ApJL, 734, L24

de Heij, V., Braun, R., & Burton, W. B. 2002, A&A, 391, 159

Dennison, B., Simonetti, J. H., & Topasna, G. A. 1998, PASA, 15, 147

Draine, B. T. 2011, *Physics of the Interstellar and Intergalactic Medium, ed. B. T. Draine* (Princeton Univ. Press)

Faridani, S., Flöer, L., Kerp, J., & Westmeier, T. 2014, A&A, 563, A99

Finkbeiner, D. P. 2003, ApJS, 146, 407

Gibson, S. J., Koo, B., Douglas, K. A., et al. 2012, American Astronomical Society Meeting Abstracts, 219, #349.29

Haffner, L. M., Reynolds, R. J., Tufte, S. L., et al. 2003, ApJS, 149, 405

Heiles, C. 1979, ApJ, 229, 533

Heiles, C. 1984, ApJS, 55, 585

Heitsch, F., & Putman, M. E. 2009, ApJ, 698, 1485

Heitsch, F., Bartell, B., Clark, S. E., et al. 2016, arXiv:1606.06689

Jin, S. 2010, MNRAS, 408, L85

Kang, J.-h., & Koo, B.-C. 2007, ApJS, 173, 85

Kamphuis, J., Sancisi, R., & van der Hulst, T. 1991, A&A, 244, L29

Koo, B.-C., Heiles, C., Stanimirović, S., & Troland, T. 2010, AJ, 140, 262

Kwak, K., Shelton, R. L., & Raley, E. A. 2009, ApJ, 699, 1775

Levine, E. S., Blitz, L., & Heiles, C. 2006, ApJ, 643, 881

McClure-Griffiths, N. M., Dickey, J. M., Gaensler, B. M., & Green, A. J. 2002, ApJ, 578, 176

Mirabel, I. F., & Morras, R. 1990, ApJ, 356, 130

Plöckinger, S., & Hensler, G. 2012, A&A, 547, AA43

Putman, M. E., de Heij, V., Staveley-Smith, L., et al. 2002, AJ, 123, 873

Putman, M. E., Saul, D. R., & Mets, E. 2011, MNRAS, 418, 1575

Putman, M. E., Peek, J. E. G., & Joung, M. R. 2012, ARA&A, 50, 491

Rhode, K. L., Salzer, J. J., Westpfahl, D. J., & Radice, L. A. 1999, AJ, 118, 323

Santillán, A., Franco, J., Martos, M., & Kim, J. 1999, ApJ, 515, 657

Tamanaha, C. M. 1997, ApJS, 109, 139

Tenorio-Tagle, G. 1980, A&A, 88, 61

Tenorio-Tagle, G., Franco, J., Bodenheimer, P., & Rozyczka, M. 1987, A&A, 179, 219

Voges, W., Aschenbach, B., Boller, T., et al. 1999, A&A, 349, 389

Wakker, B. P. 1991, A&A, 250, 499

Wakker, B. P., & van Woerden, H. 1991, A&A, 250, 509

Wakker, B. P. 2004, Ap&SS, 289, 381

Westmeier, T., Brüns, C., & Kerp, J. 2005, A&A, 432, 937

Winkel, B., Ben Bekhti, N., Darmstädter, V., et al. 2011, A&A, 533, A105

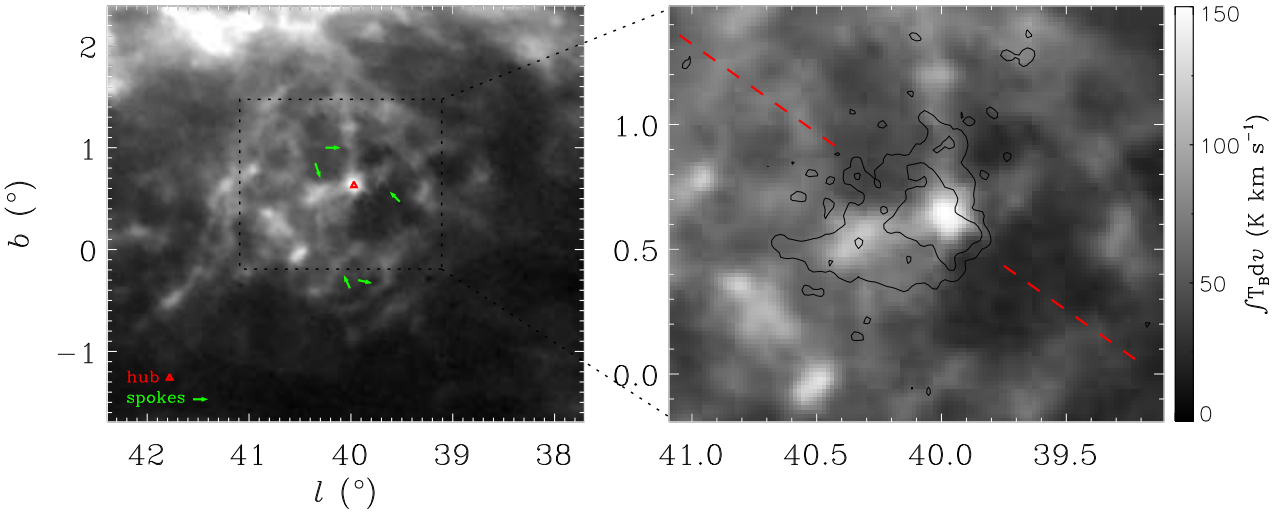

Figure 1. HI integrated-intensity maps of the overall picture of the supershell GS040 (left) and a close-up view inside its ring structure (right). The maps are obtained by integrating the emission between $v_{\rm LSR} = -141$ and -66 km s^{-1}. The features described in Sec. 2 are labeled in the left image. The overlaid contours in the right image show the overall appearance of the high-velocity cloud CHVC040 in integrated HI emission (see Figure 4). The position-velocity diagram in Figure 3 was obtained along the dashed red line.

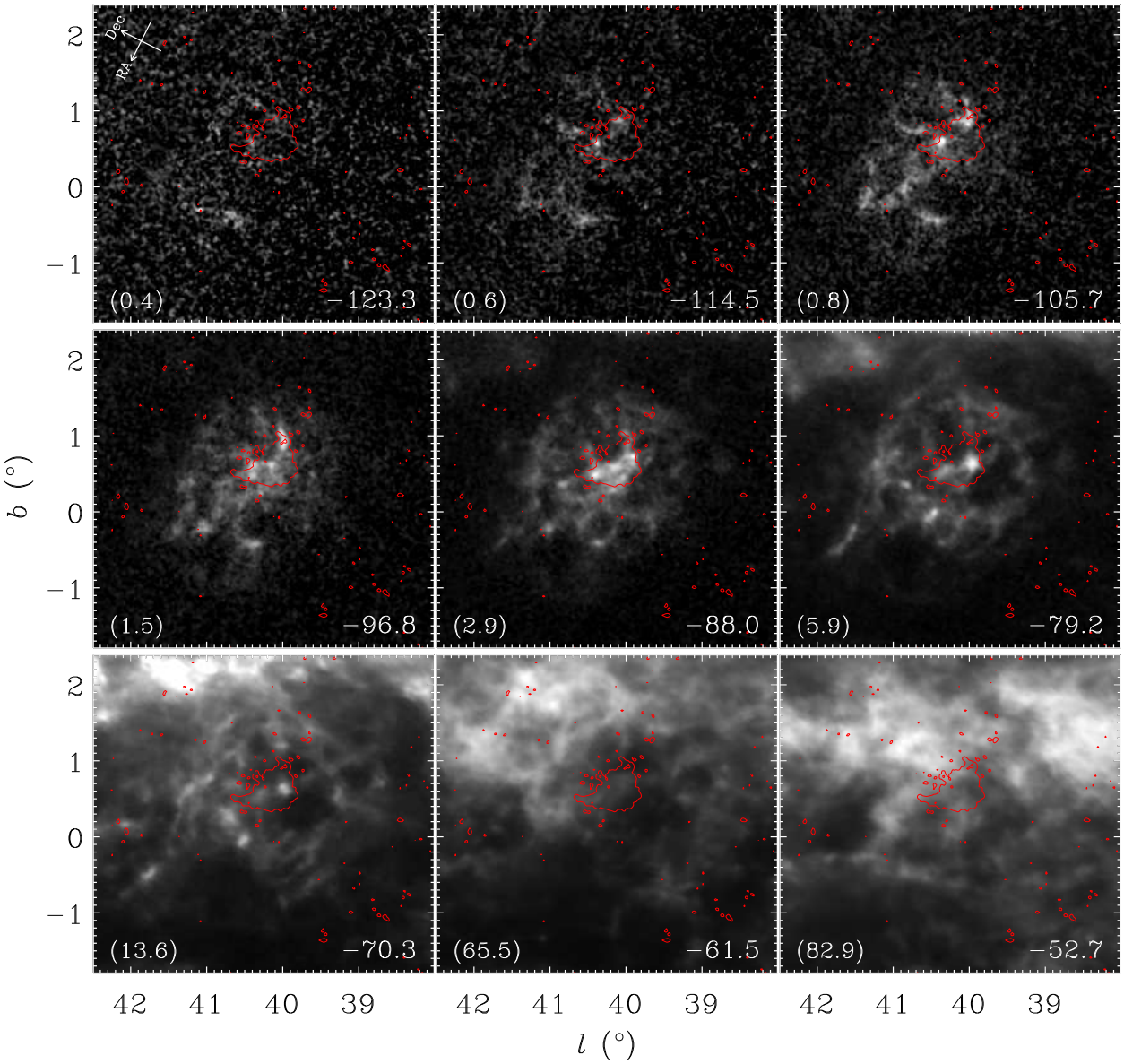

Figure 2. Velocity-channel maps of GS040 in the HI data. The central LSR velocity of each channel is written at the bottom right corner in $\mathrm{km\,s^{-1}}$. The channel width and interval are 3.68 and 5.15 $\mathrm{km\,s^{-1}}$, respectively. The HI brightness temperature in gray scale ranges from 0 K (black) to the value (white) in parentheses at the bottom left corner of each panel in Kelvins. Contours show the overall appearance of CHVC040 in integrated HI emission (see Figure 4). To aid comparison to literature studies in Equatorial coordinates, arrows are shown in the first panel indicating Right Ascension and Declination (J2000) coordinate directions.

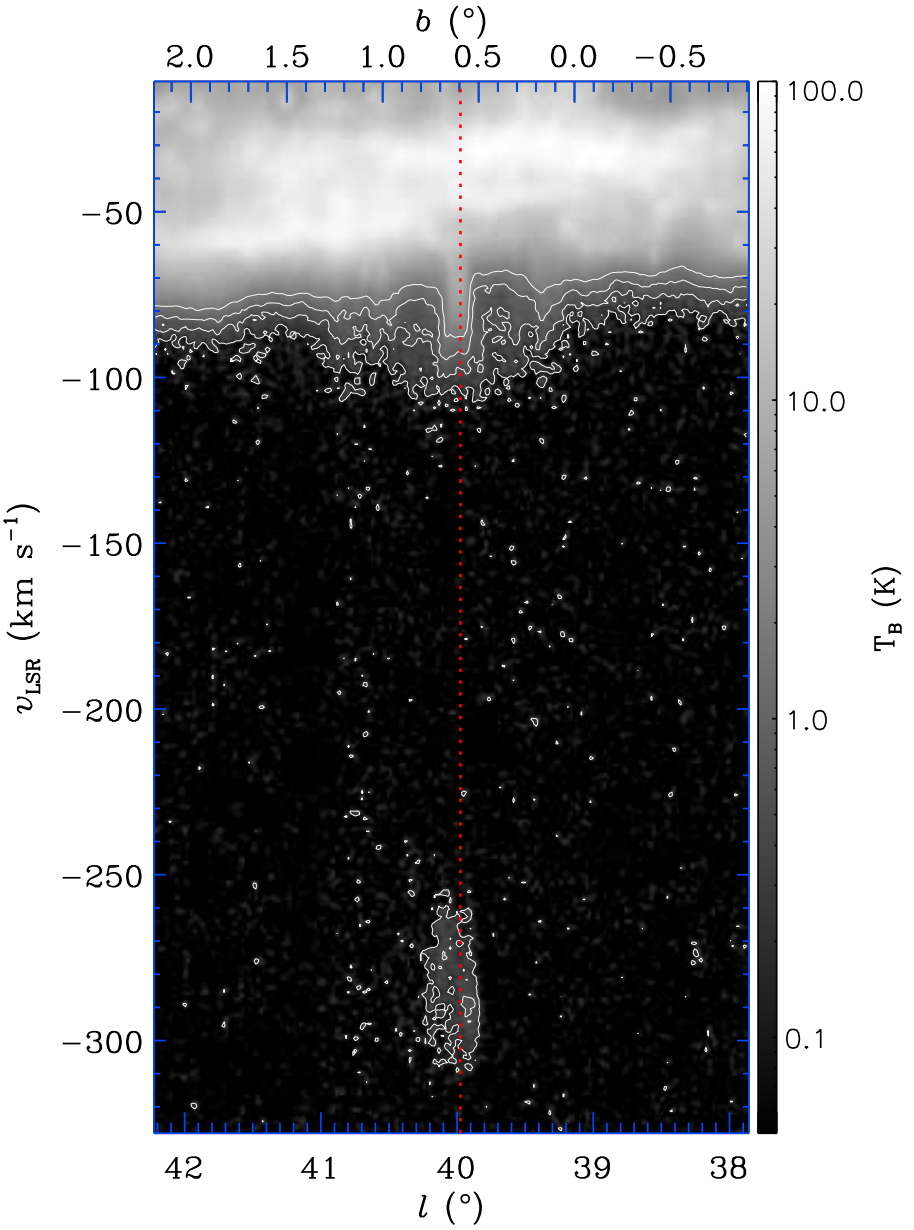

Figure 3. Position-velocity map of HI emission of GS040 and CHVC040. This diagram is drawn along a line crossing the center of GS040 at position angle of about 35° (Figure 1). The lower and upper x-axis indicate ℓ and b coordinates of the position, respectively. The y-axis indicates the LSR velocity. The contour levels are 0.2, 0.5, 1, and 2 K in brightness temperature. The dotted vertical line is toward the center of GS040.

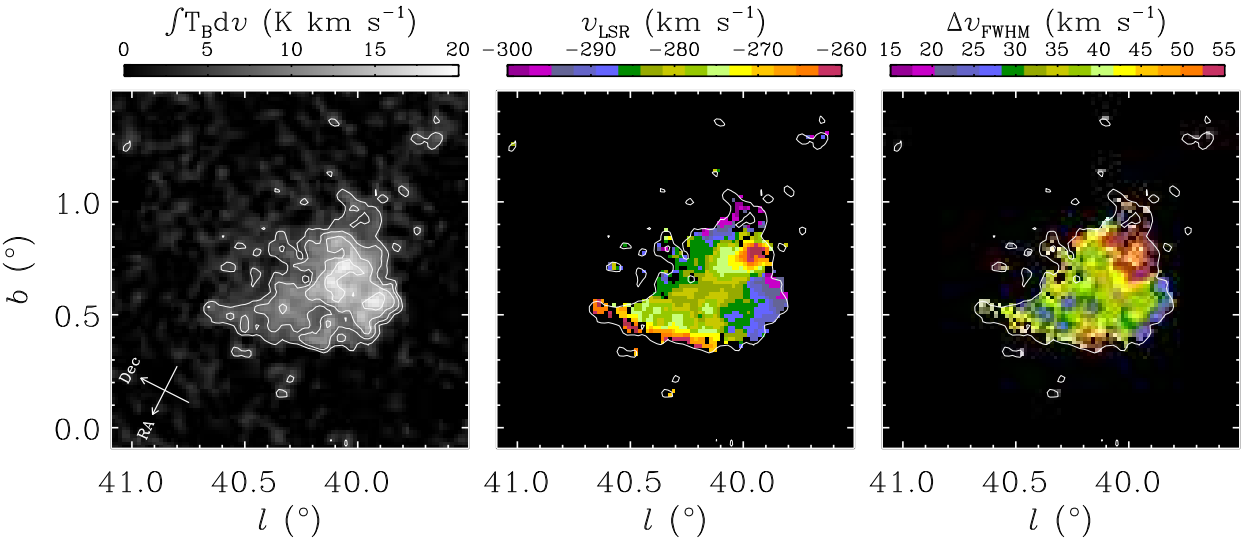

Figure 4. Spatial and velocity structures of the high-velocity cloud CHVC040. *Left:* HI intensity map integrated over LSR velocities from −330 to −230 km s^{-1}. Contours are drawn at 5, 8, 12, and 16 K km s^{-1}. If the emission is optically thin, 1 K km s^{-1} corresponds to hydrogen columns of 1.82×10^{18} cm^{-2}. *Middle and Right:* Central velocity and velocity width maps derived by fitting single Gaussian curve to each line profile. The fit is limited to positions with integrated intensity greater than 5 K km s^{-1}, i.e., within the white contour. The pixels where the emission is weak and a reasonable fit cannot be obtained are also blanked out. To aid comparison to literature studies in Equatorial coordinates, arrows are shown in the left panel indicating Right Ascension and Declination (J2000) coordinate directions.

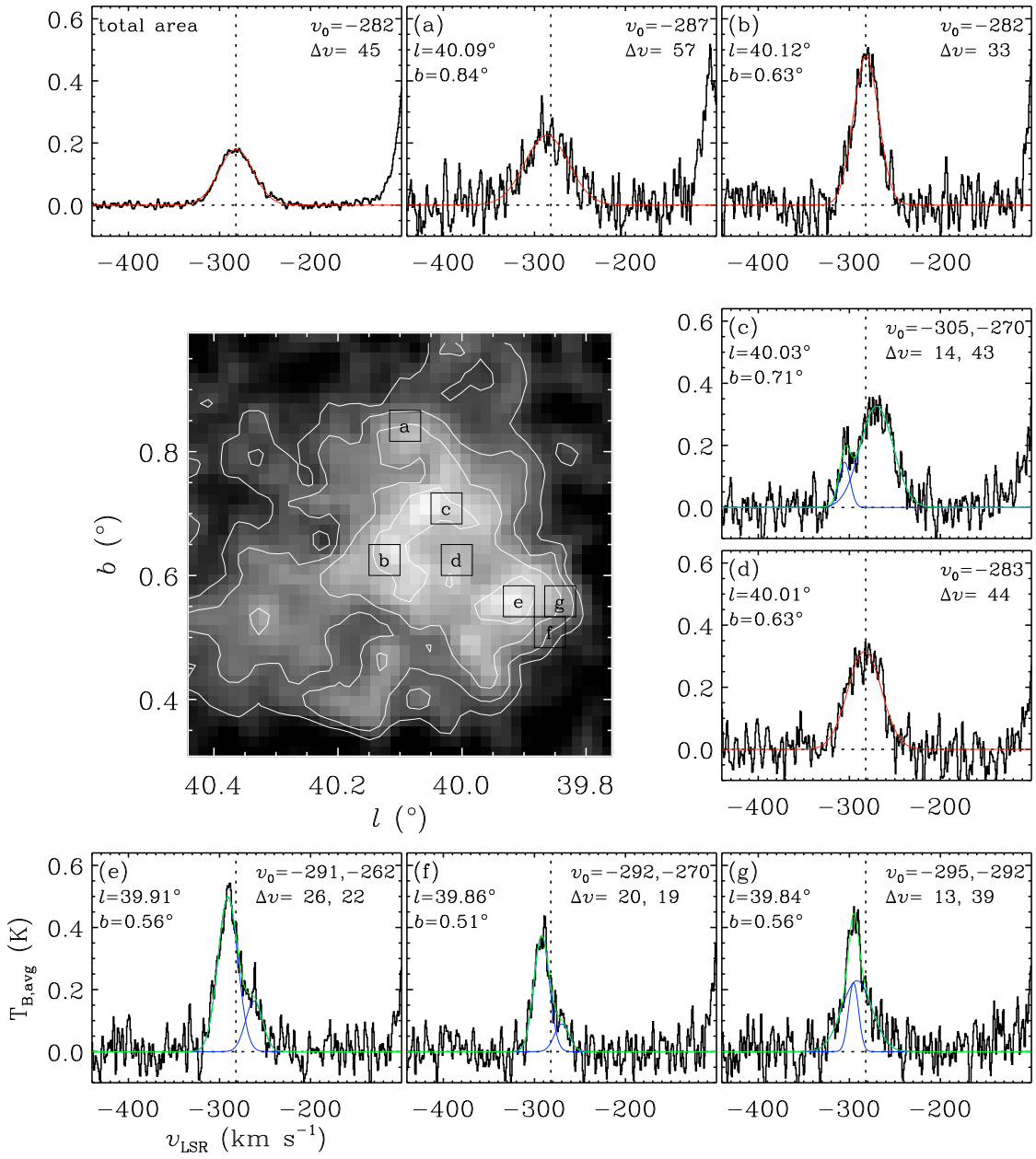

Figure 5. Examples of CHVC040 HI line profiles. The profile in the top left frame is an average profile of the whole cloud. The rest of line profiles are extracted from the areas marked by boxes in the central image, which is the integrated intensity map in Figure 4. The profiles have been Hanning smoothed to have a velocity resolution of 2.96 km s^{-1}. A Gaussian fit with the suitable number (n) of components is applied and displayed with a red (n=1) or green curve (n=2; each in a blue line). Resultant parameters, including central LSR velocity (v_0) and velocity width (Δv) in km s^{-1}, are written on the top right corner of each panel. A vertical line at the central velocity of the average line profile (−282 km s^{-1}) is drawn to aid the intercomparison of different plots.